Published by
NIGERIAN SOCIETY OF PHYSICAL SCIENCES
Available online @ https://journal.nsps.org.ng/index.php/jnsps

J. Nig. Soc. Phys. Sci. 5 (2023) 1386

Journal of the Nigerian Society of Physical Sciences

Experimental and computational studies of the corrosion inhibitive effects of *Zingiber officinale* rhizomes on mild steel corrosion in acidic solutions

C. B. Adindu[a,*], S. C. Nwanonenyi[b], C. B. C. Ikpa[a]

[a]*Department of Chemistry, Imo State University, P.M.B 2000 Owerri, Imo State, Nigeria*
[b]*Department of Polymer and Textile Engineering, Federal University of Technology, P.M.B.1526, Owerri, Nigeria*

Abstract

The study investigates the anticorrosion potentials of *Zingiber officinale* (ZO) on mild steel induced in 1.0 M HCl and 0.5 M H_2SO_4 acid solution respectively using structural characterization (gas chromatography-mass spectroscopy, GC-MS and Fourier transform infrared spectroscopy, FTIR) and electrochemical (electrochemical impedance spectroscopy, EIS and potentiodynamic polarization, PDP) techniques respectively and theoretical simulations. The structural characterization was performed to identify chemical constituents and functional groups present in the plant extract whereas electrochemical techniques and theoretical computations were used to examine the anticorrosion potentials of the extract and validate the experimental results. The GC-MS result revealed the presence of twenty-three (23) compounds within the extract and out of which three (1-(1,5-dimethyl-4-hexenyl)-4-methyl-, dodecanoic acid and 9-Octadecenoic acid (Z)-2-hydroxy-1-(hydroxymethyl)ethyl ester) were selected for computational simulation and the results of FTIR revealed the presence of the following functional groups (O–H, C=C, C=O, C–C and C–H) in the ZO extract. The results of EIS revealed that extract of ZO exhibited corrosion inhibition efficieny of 82.7% and 93.6 % for mild steel in 1 M HCl and 0.5 M H_2SO_4 solution respectively at maximum inhibitor concentration of 1000 mg/L for mild steel. Also, PDP results revealed that ZO extract functioned as mixed inhibitor because both the anodic and cathodic reaction process was altered. The quantum chemical calculation results revealed that 9- Octadecenoic acid (Z)-2-hydroxy-1-(hydroxymethyl) ethyl ester had a good energy gap (ΔE) compared to other two compounds, indicating its better adsorption interaction with the metal surface in sulfuric acid environment. This was further confirmed by its good adsorption energy of -355.55 Kcal/mol with mild steel surface in H_2SO_4 environment compared with -167.81Kcal/mol in HCl environment from the molecular dynamic simulation.

DOI:10.46481/jnsps.2023.1386

Keywords: *Zingiber officinale,* solvation molecules, corrosion, molecular dynamic simulation, inhibition efficiency

Article History :
Received: 06 February 2023
Received in revised form: 19 May 2023
Accepted for publication: 12 June 2023
Published: 23 August 2023

Communicated by: K. Sakthipandi

1. Introduction

Corrosion of component tools and parts made of metallic alloys in different service environments and its control is a vital research area and requires adequate attention due to its utmost importance in industrial and engineering sectors. Thus,

*Corresponding author tel. no: +234 7030676855
Email address: blessingojiegbe@yahoo.com (C. B. Adindu)

purified metals together with their alloys possess some inherent features and exhibit outstanding performances in different service environment to ensure sustainable economy. Corrosion of metals is an unpreventable phenomenon caused by unfavourable interactions between the metal substrate and its environment surrounding and the interaction is electrochemical in nature involving anodic and cathodic process. Metals and their alloys are indispensible materials for the design and fabrications of water treatments plants, heat exchangers, dye-bath, drill bits, food processing equipment, hollow pipes for fluid transportation, distribution and storage, etc. filter membrane, etc. However, it is observed over time that scales of inorganic materials or products develop on the internal walls of these components and reduced the efficiency or productivity. On the other, removing these unwanted products via acid cleaning or acidizing process with dilute mineral acids (hydrogen chloride and sulphuric acid) is ideal but significant corrosion effects are introduced on the metal surface on the process.

The resultant effects of metal corrosion are enormous; it causes tremendous damage to life-span and integrity of industrial tools of metallic component especially in oil and gas sectors and other chemical processing industries [1-3], creates pollution problems which poses great health challenge to man and his environment and results to waste of economic resources in routine corrective and preventive maintenance and material loss. Thus, identifying the possible solution to mitigate these problems associated with metal corrosion is imperative and highly efficient corrosion inhibitors from organic sources together with computational modeling techniques possess all it will take to achieve this feat.

Many researchers in the field of corrosion of metals and their inhibition have reported the use of several methods to combat the problem of corrosion of metals in different service environment [4]. One of such methods is the use of material regarded as corrosion inhibitor and it is not a complex technique neither does it requires much training during application. Corrosion inhibitor is a material capable of reducing the corrosive effect of any corrodent system when added in a little amount or quantity. Many corrosion inhibitors in use during metal corrosion and its control are sourced from either organic or synthetic background with little or no modification. Chromates, some imidazole based inhibitors, etc. are typical examples of corrosion inhibitor from synthetic sources with effective performance but the application of these inhibitors are currently restricted due to their toxicity and other environmental issues.

Over time, the use of extracts from various plant leaves, bark, root, etc. has received detailed attention as anti-corrosion material. Some of these natural materials particularly plant materials, proteins, biopolymer and amino acids have been reported to function as effective corrosion preventing additives [5-10]. Plant materials are viewed to contain rich chemical compounds that can be extracted by simple methods and some of these chemicals are known to resemble the synthetic organic corrosion retarding compounds and have been proven to function as effective as their synthetic counterparts. These materials have at different proportions hetero atoms which contain sulphur, nitrogen and oxygen in a conjugation as well as double bond and aromatic ring in their chemical structures [11-20]. It is believed that these functional groups within the chemical structure of inhibitor play significant roles in corrosion, adsorption and inhibition. *Zingiber officinale* (ginger) plays a very important role in medicinal science and it has high medicinal value due to its antifungal, anti-bacterial and other nutritional benefits. Thus, it has been in use in many parts of the world as remedy and cure for many known diseases [21-22]. This study is aimed at investigating the corrosion inhibitive effects of ZO ethanol extract on mild steel corrosion in acidic solutions using experimental and theoretical studies respectively. The essence of employing the computational study in the study is to unravel the correlation existing between the inhibitor efficiency and their electronic molecular structures. Furthermore, the work seeks to widen the application of ginger as eco-friendly corrosion inhibitor for mild steel protection [23-25].

2. EXPERIMENTAL SECTION

2.1. Preparation of materials

The metal used for the research was mild steel low carbon grade with the following composition: 0.05%C, 0.36%P, 0.03%Si, 0.6%Mn and 98.96%Fe. The metal coupons were cut to 3 x 3 x 0.14 cm using mechanical cutter, cleaned, polished with fine emery paper (1000 and 1200 grade) degreased and prepared as earlier described in our previous work [26]. *Zinbiber officinale* rhizomes tuber used was obtained from harvested samples kept at Agricultural farm store in Imo state polytechnic Umuagwo, Imo State and identified at Crop Science Laboratory, Federal University of Technology Owerri, Imo state. The ZO tuber foreskin was washed thoroughly with water to remove dirts, pealed to remove the thick back, sliced into pieces, dried thoroughly, pulverized to fine powder particle, stored in an air tight container and kept for corrosion studies. The prepared ZO sample (50 g) was introduced in 500 ml of absolute ethanol in a beaker and allowed to stand for 72 h and kept in an aerated condition. The mixture was thoroughly filtered with filter paper and the solution obtained was used to prepared inhibited solution for corrosion studies.

The stock blank of 1 M HCl and 0.5 M H_2SO_4 acid solution respectively was prepared using dilution serial principle whereas the inhibited solutions were prepared by introducing 200 and 1000 mg of ZO extract respectively into 1 L of 1 M HCl and 0.5 M H_2SO_4 acid solution, respectively.

The prepared ZO extract sample was concentrated with rotary evaporator and subjected for functional group examination and analysis in a Fourier transform infrared (FTIR) spectrophotometer (Nicolet Magna-IR 560 model)[28].

Also, the prepared ZO powdered sample was subjected to Gas chromatography-mass spectrophotometer, GC-MS

(19091S-433UI model) for examination and analysis. The HP-5ms Ultra Inert 0°C - 325°C: with dimension 30 m × 250 μm × 0.25 μm was used for the GC-MS analysis, at the gas Chromatography section, the oven temperature was 50 °C, held for 120 secs raised to 180 °C at a rate of 50 °C/min the final temperature was 325 °C with injection volume of 10 μL and 7.3614 psi pressure. The carrier gas was Helium with flow rate of 0.97414 mL/min, For mass Spectrometer part. The solvent was methanol and the scanning was at 40-650 m/z the result obtained was compared with NIST mass spectral library search program.

2.2. *Electrochemical experiments*

(a) Electrochemical experiments were done using direct current voltammetry (VERSASTAT 400) advanced electrochemical workstation. The corrosion cell is made of cylindrical glass and contains three conventional electrodes namely [7]; working electrode (mild steel coupon), graphite rod (counter electrode) and reference electrode (saturated calomel electrode). The working electrode, a mild steel coupon of dimension 1.5 cm × 1.5 cm was affixed in polytetrafluoroethylene (PTFE) rods using epoxy resin in a way that just one of its surfaces of area 1 cm ^{2} was exposed to test solution under evaluation. The electrochemical workstation, central processing system, monitor and electrolytic cell terminals were connected tightly with luggin capillaries. Open circuit potential (OCP) was performed for the test solution to achieve steady state potential at 1800 secs and 303 K before the EIS and PDP experiments commenced. The measurements were performed at the end of 1800 secs in an aerated environment and stagnant test solution. Polarization curves were determined from the scanning electrode potential of -250 mV to +250 mV versus corrosion potential (Ecorr) at a scan rate of 0.33 mV/s [29] while linear polarization segments of cathodic and anodic curves were extrapolated to determine corrosion current densities (i_{corr}) using V^3 studio software.

Electrochemical impedance measurements were undertaken at corrosion potential (E_{corr}) at a frequency range of 10 m Hz to 100 kHz and amplitude of perturbation of 5 mV. Electrochemical data were analyzed using the ZSim Win 3.10 software modeling package. The experimental measurements (i.e both EIS and PDP) were repeated three different times to ensure reproducibility of results. EIS measurement was performed to monitor the effect of thin film of the active inhibitor components adsorbed on the metal surface while PDP measurement was performed to proof evidence of effect of inhibitor on cathodic and anodic partial reactions and this assists to classify whether the inhibitor acts as cathodic, anodic or mixed type inhibitor.

2.3. *Theoretical computations*

The results of corrosion studies revealed that ethanol ZO extract retarded the corrosion of mild steel in the different acid solution medium studied and theoretical computations was used to validate the experimental results. The theoretical studies provide evidence of chemical parameters within the inhibitor structures that are responsible for the corrosion inhibition and also give information on the adsorption energy between the corrosion inhibitor species and metal surface. Molecular geometries and electron distributions influencing corrosion inhibition properties of some materials known had been previously evaluated using density functional theory [30 - 32]. Structures of the most three (3) active constituents of the ginger rhizomes were selected from the GC-MS results and modeled. The theoretical calculation was done with Material Studio software Accelrys (7.0 version) within the framework of density functional theory (DFT) tools (quantum chemical computation and molecular dynamic simulation) from the molecular point of view.

3. RESULTS AND DISCUSSION

3.1. *Sample characterization*

3.1.1. *FTIR Result*

The FTIR characterization was performed to ascertain the functional groups present in the extract of ZO which may have facilitated its adsorption on the mild steel surface. The result obtained is presented in Figure 1. The prominent peaks observed in the Figure include; a strong and broad hydrogen bonded (O – H) stretching band at 3272.6 cm^{-1}, the strong band at 1640.0 cm^{-1} may be assigned to C = C and C = O stretching vibrations which may be due to the presence of conjugation in the chemical constituents of the ZO powder and the band at 1408.6 cm^{-1} which corresponds to the C – H bending bands of CH_2 and CH_3 groups and the absorption bands at 1043.7 – 1084.7 cm^{-1} which may be assigned to C – O functional group [34]. The FTIR result revealed that the extract contain functional groups which may facilitate the effectiveness of the extract to adsorb and interact with the mild steel surface. As a result, protection of the metal surface may be as a result of the adsorption of these functional groups present in the ZO powder [35].

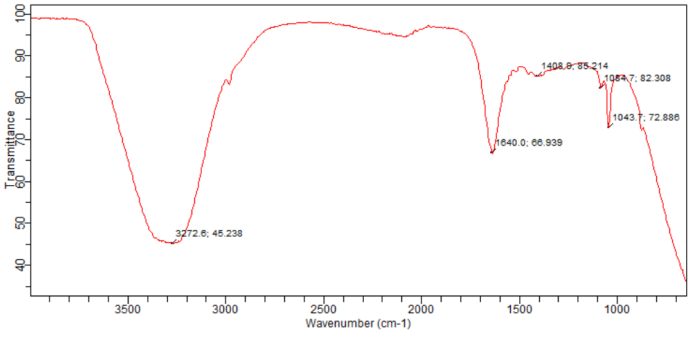

Figure 1: FTIR image of ZO powder

3.1.2. *GC-MS Results*

The active phytochemical components of ZO [36] were revealed in the Gas Chromatography-Mass Spectroscopy result presented in Table 1 and Figures 2 & 3. The peaks were identified by comparing their retention times with those found in (NIST-MS) library. Compounds with less than 4 % area

peak were not included in the presented result. Benzene, 1-(1,5-dimethyl-4-hexenyl)-4-methyl-, Dodecanoic acid and 9-Octadecenoic acid (Z)-2-hydroxy-1-(hydroxymethyl) ethyl ester were selected for the computational studies.

3.2. Electrochemical Results

Potentiodynamic polarization (PDP) and electrochemical impedance spectroscopy (EIS) experiments were carried out to understand the effect of ZO extract on the corrosion of mild steel in acidic environments. The concentrations of the ZO extract chosen for the experiment were 200 and 1000 mg/L respectively and the plots of OCP obtained in 1.0 M HCl and 0.5 M H_2SO_4 environments are presented in Figure 4 (a & b).

3.2.1. Electrochemical impedance spectroscopy results

Impedance experiments were undertaken on mild steel in the selected acid solutions in the presence and absence of ZO inhibitor at two concentrations. The Nyquist and Bode plots respectively for mild steel corrosion in 1 M HCl and 0.5 M H_2SO_4 acid solution respectively are presented in Figures 5 (a & b) and 6 (a & b) respectively while the electrochemical parameters from the EIS experiments are presented in Table 2. The Nyquist plot can be seen to show a single depressed semicircle in the region of high frequency for all the systems studied equivalent to one time constant found in the bode graphs. In the Nyquist plot, the high frequency that intercepts with the real axis in named the solution resistance (R_s) whereas the low frequency that intercept with the real axis is called the charge transfer resistance (R_{ct}) [37]. The impedance results were fitted into an equivalent circuit model $R_s\,(Q_{dl}R_{ct})$ to get the impedance data presented in Table 2 and Q_{dl} is the double layer capacitance. This equivalent circuit has been previously used to model impedance result [38-39] for mild steel corrosion in acidic media. The solution resistance in the equivalent circuit was shorted by a constant phase element (CPE) which was subsequently connected parallel to the charge transfer resistance (R_{ct}). The pure capacitor was replaced in the equivalent circuit to account for the deviations from ideal dielectric behavior which may arise from the dissimilar nature of the electrode surfaces. The electrochemical impedance response of the constant phase element is given in equation (1):

$$Z_{CPE} = Q^{-1}\,(J\omega^{-n})\,. \tag{1}$$

Here Q is the CPE constant, n is the CPE exponent, J an imaginary number which is equivalent to $(-1)^{1/2}$ and ω is the angular frequency in s^{-1} ($\omega = 2\pi f$), f is the frequency in Hz. The inhibition efficiencies presented in Table 2 from the impedance response were estimated according to the equation (2):

$$IE\% = \left(1 - \frac{R_{ct,\,bl}}{R_{ct,\,in}}\right) \times 100, \tag{2}$$

where $R_{ct,bl}$ represents charge transfer resistance in the absence of the inhibitor and $R_{ct,\,in}$ represents charge transfer resistance when the inhibitor was added. The results presented in Table 2 shows that R_{ct} values increased with increase in the concentration of the ZO inhibitor whereas the Q_{dl} values decreased as the ZO concentration increased, the former action indicated that anticorrosion process is experienced whereas the later showed that the ZO extract actually adsorbed on the mild steel surface.

3.2.2. Potentiodynamic Polarization (PDP) Results

The mechanisms of the partial anodic and cathodic half corrosion reactions as well as the effect of ZO on either reactions were studied with the aid potentiodynamic polarization experimental techniques. Figure 7 shows the PDP plots for mild steel corrosion in (a) 1 M HCl solution and (b) 0.5 M H_2SO_4 acid solutions with and without ZO inhibitor and Table 3 shows the PDP parameters for mild steel corrosion in the presence and absence of the inhibitor. The result in Table 3 shows that the addition of the inhibitor reduced the anodic and also the cathodic half corrosion reactions while shifting the corrosion reaction potential (E_{corr})towards the negative value as well as reducing both the anodic and cathodic current densities in both acidic environments. These effects showed that ZO functioned as a mixed type corrosion inhibitor for mild steel in both acidic solutions. The corrosion inhibition efficiencies (IE%) reported for ZO were estimated from the current densities without ($i_{corr,bl}$) and with ($i_{corr,inh}$) ZO inhibitor according to the equation (3):

$$IE\% = \left(1 - \frac{i_{corr,\,inh}}{i_{corr,\,bl}}\right) \times 100. \tag{3}$$

The ($IE\%$) values shown in Table 3 are remarkably high indicating that ZO is a good anti-corrosion material.

3.3. Theoretical computational results

3.3.1. Quantum chemical computation:

Exact experimental identification of contributions of the individual constituents of the bulk extract to the overall corrosion inhibition has been hindered as a result of the complex nature of the plant extract, we therefore rely on quantum chemical computations as well as molecular dynamic simulations to ascertain the individual contributions of three selected major constituents of ZO extract to the experimentally observed corrosion inhibition effects. The molecular structures of benzene, 1-(1,5-dimethyl-4-hexenyl)-4-methyl- (α-Curcumene), dodecanoic acid (Lauric acid) and 9-Octadecenoic acid (Z)-, 2-hydroxy-1-(hydroxymethyl)ethyl ester present in the ZO were optimized with the density functional theory electronic program DMol3 utilizing a Mulliken population analysis [40, 41). Electronic condition for the simulation are restricted spin polarization by the DND basis set and the Perdew–Wang (PW) local correlation density functional, Further calculation was achieved to obtain the quantum chemical parameters such as the lowest unoccupied molecular orbital energy (E_{LUMO}) the highest occupied molecular orbital energy (E_{HOMO}), energy gap (ΔE), absolute hardness (η), chemical softness (σ), the fraction of electrons that were transferred from inhibitor molecule to the metal surface (ΔN) and fukui functions. To mimic the extraction medium, these calculations were done in the presence of ethanol as the solvated medium using LDA and PWC functional.

Table 1: Some of the active components of ZO from the GC-MS result

Peak No.	Retention Time	Name of compound	Molecular weight (g/mol)	Molecular formular	Area percent
11	16.6262	Benzene, 1-(1,5-dimethyl-4-hexenyl)-4-methyl-	202.3352	$C_{15}H_{22}$	4.1746
13	17.0368	1,3-Cyclohexadiene, 5-(1,5-dimethyl-4-hexenyl)-2-methyl-, (Zingiberene)	204.3511	$C_{15}H_{24}$	4.6564
18	19.6874	Dodecanoic acid (Lauric acid)	200.32	$C_{12}H_{24}O_2$	5.414
23	23.8033	Tetradecanoic acid	228.37	$C_{14}H_{28}O_2$	5.2783
35	27.7678	n-Hexadecanoic acid	256.40	$C_{16}H_{32}O_2$	4.6996
41	29.9013	9,17-Octadecadienal, (Z)-	264.40	$C_{18}H_{32}O$	5.0745
55	32.8447	9-Octadecenoic acid (Z)-, 2-hydroxy-1-(hydroxymethyl)ethyl ester	356.50	$C_{21}H_{40}O_4$	16.4469

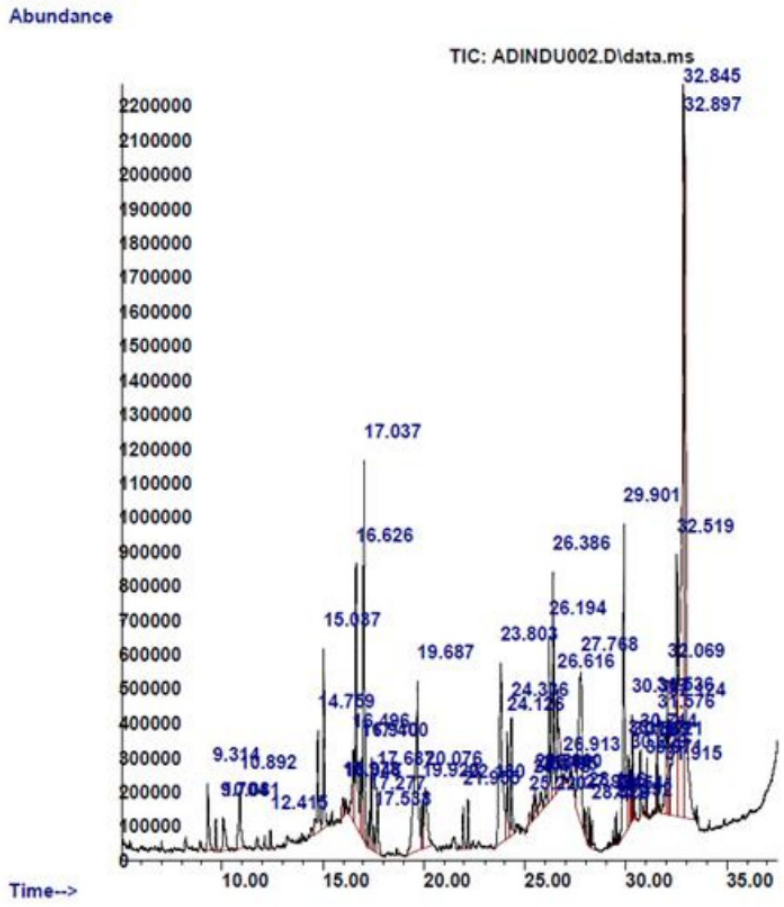

Figure 2: GC-MS microgram of ZO powder

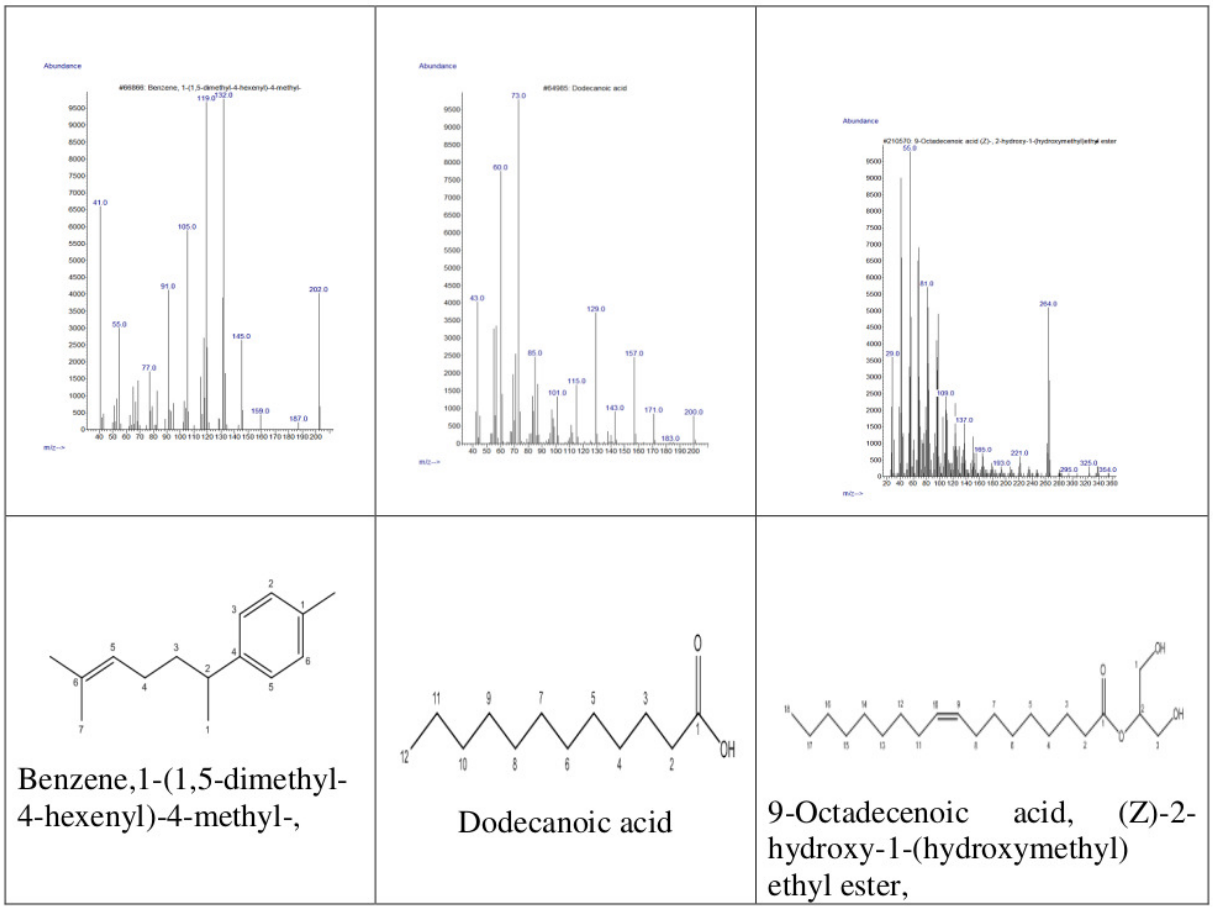

Figure 3: Mass spectra and molecular structures of the some ZO constituents

Table 2: Electrochemical impedance parameters for mild steel corrosion with and without ZO

System	Rs (ω cm^2)	R_{ct} (Ω cm^2)	N	Q_{dl} (μF cm^{-2})	IE%
1 M HCl	1.67	104	0.88	91.7	
200 mg/L ZO	1.78	286	0.89	38.9	63.6
1000 mg/L ZO	1.81	602	0.89	22.3	82.7
0.5 M H_2SO_4	2.87	8.4	0.84	258.8	
200 mg/L ZO	3.16	40	0.89	153.6	79
1000 mg/L ZO	3.26	132	0.89	61.5	93.6

Table 3: Potentiodynamic polarization parameters for mild steel corrosion with and without ZO inhibitor

System	E_{corr} (mV vs SCE)	I_{corr} (μA/cm^2)	b_a (mV dec^{-1})	b_c (mV dec^{-1})	IE%
1 M HCl	-471.3	649.4	126.3	168.5	
200 mg/L ZO	-477	224.5	112.7	123.2	65.4
1000 mg/L ZO	-474.3	109.6	104.8	116.9	83.1
0.5 M H_2SO_4	-500	2940	136.7	208.5	
200 mg/L ZO	-506	1476	123.5	194.7	49.8
1000 mg/L ZO	-509	756.9	114.3	186.2	74.3

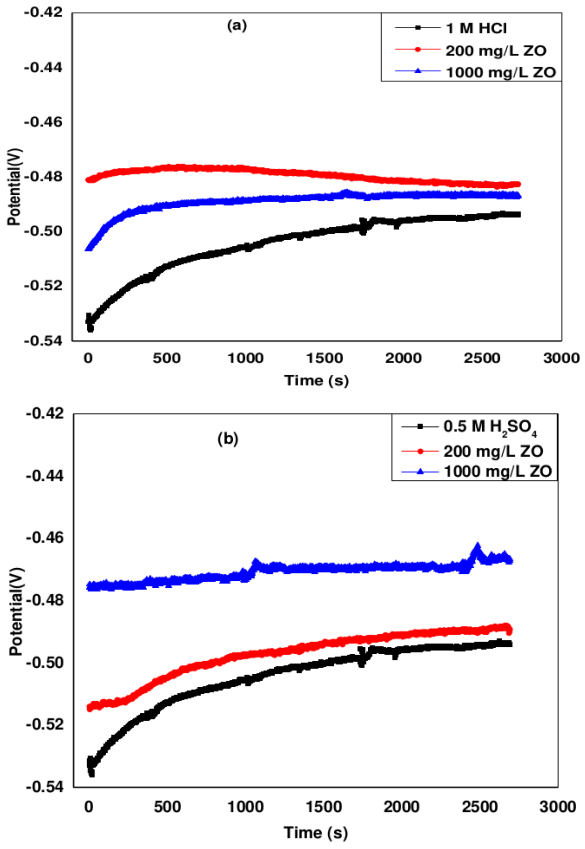

Figure 4: Graph of open circuit potential for mild steel in (a) 1 M HCl (b) 0.5 M H_2SO_4 in the presence and absence of ZO.

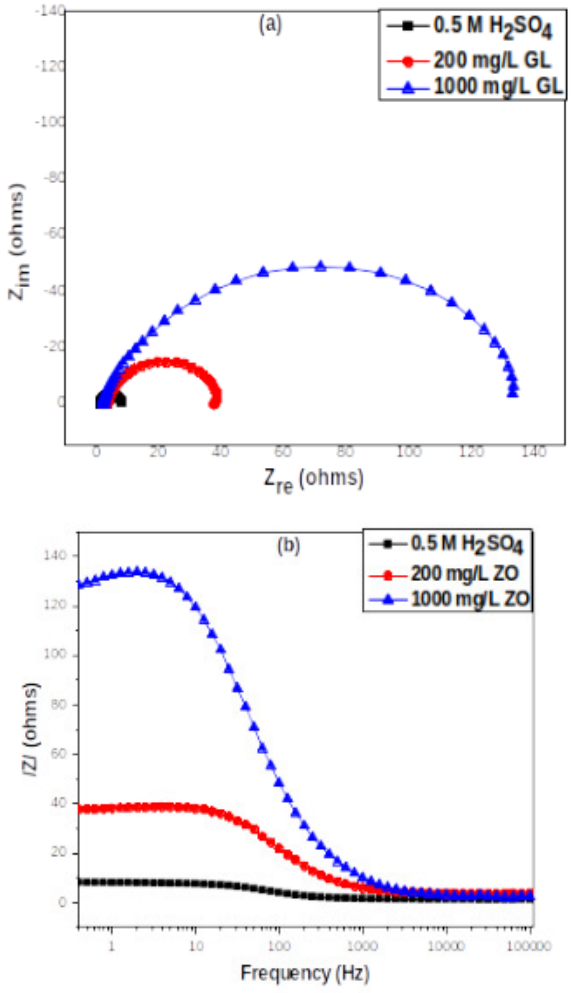

Figure 5: Nyquist and Bode plots for mild steel corrosion without and with the ZO extract in 0.5 M H_2SO_4

The simulation results including the optimized structure, frontier orbitals (HOMO and LUMO orbital), the Fukui indices (f^+ and f^-) and the electron density are shown in Figure 8 while the quantum chemical parameters such as HOMO energy (E_{HOMO}), LUMO energy (E_{LUMO}), energy gap, ($\Delta E = (E_{LUMO} - (E_{HOMO})$, electron charge transfer (ΔN), absolute hardness (η), absolute electronegativity (χ) and absolute softness(η) are presented in Table 4. High values of E_{HOMO} indicate the ability of an inhibitor to donate electron the unoccupied d-orbital of the metal. Similarly, low value of the energy gap shows that the energy needed to remove the lowest occupied orbital will be small indicating that the corrosion retardation will be high. Accordingly, f^-values show the reactivity relating to electrophilic attack while the corresponding f^+ values indicate the reactivity in relation to nucleophilic attack or the ability of the metal to attract electron. The ionization potential (I) and electron affinity (A) are, respectively, related to the HOMO and LUMO energies as shown in equations (4) and (5):

$$I = -E_{\text{HOMO}} \tag{4}$$

$$A = -E_{\text{LUMO}}. \tag{5}$$

The quantification of the electron charge transfer (ΔN) from the electron rich inhibitor to the surface of the metal was done according to equation (6):

$$\Delta N = \frac{\chi_{\text{metal}} - \chi_{\text{inh}}}{2\,(\eta_{\text{metal}} + \eta_{\text{inh}})}, \tag{6}$$

where χ_{metal} and χ_{inh} represent the absolute electronegativity of the metal and inhibitor respectively whereas η_{metal} and η_{inh} are the absolute hardness of metal and inhibitor respectively. The tabulated values of ΔN were accordingly computed using theoretical values of 7 eV/mol for χ_{metal} and θ eV/mol for η_{metal} [41]. It has been previously reported that values of ΔN relate well with binding energies of corrosion inhibitors with high values favoring stronger adsorption of the inhibitor on the metal surface [42].

The values of η, χ and σ reported in Table 4 are computed according to equations (7)-(9):

$$\eta = \frac{I - A}{2} \tag{7}$$

$$\chi = \frac{I + A}{2} \tag{8}$$

$$\sigma = \frac{1}{\eta}. \tag{9}$$

Accordingly our obtained results fall within the range of values already reported for some organic corrosion inhibitors

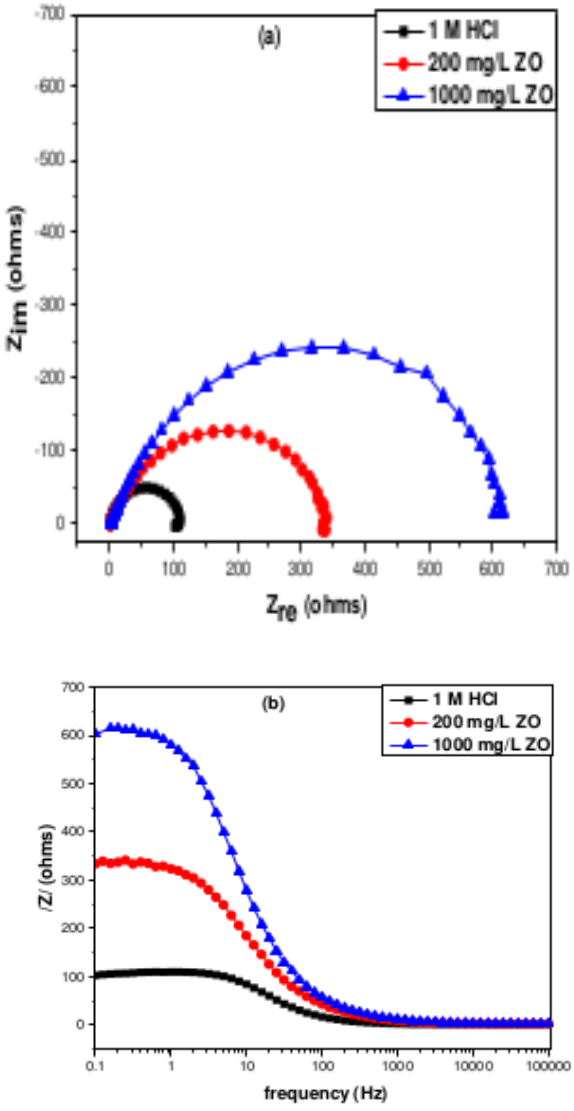

Figure 6: (a) Nyquist and (b) Bode plots for mild steel in 1.0 M HCl in the presence and absence of ZO extract

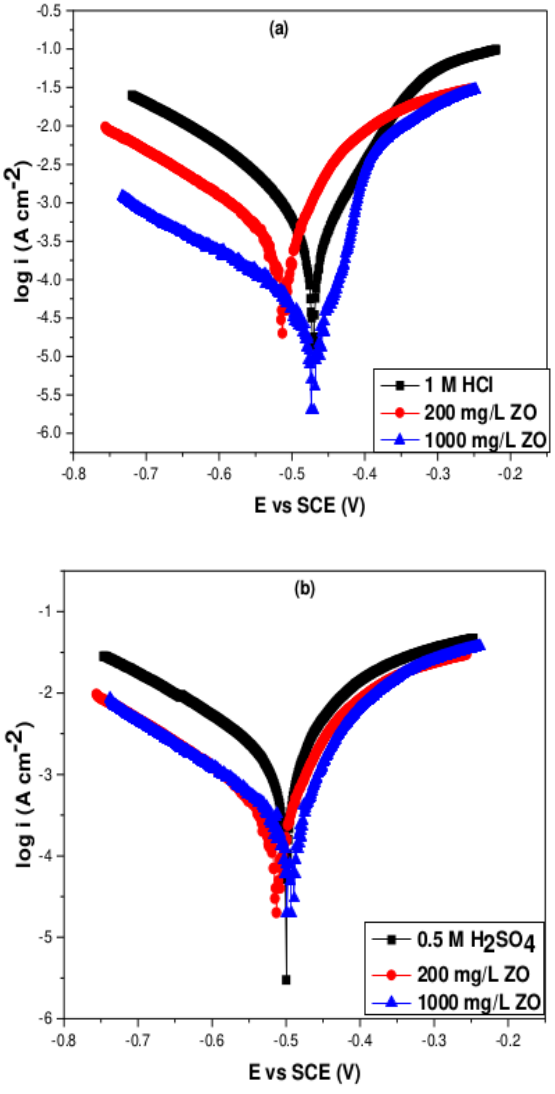

Figure 7: Potentiodynamic polarization plots for mild steel corrosion in (a) 1 M HCl and (b) 0.5 M H_2SO_4 solutions

[42]. The low value of ΔE obtained for 9-Octadecenoic acid (Z)-, 2-hydroxy-1-(hydroxymethyl)ethyl ester suggests that it must have interacted more covalently with the metal surface than the other constituents studied showing that it might have contributed more to the observed inhibiting property exhibited by the extract.

3.3.2. Molecular dynamic simulation results

Molecular dynamic simulation was performed on the three compounds previously selected using the forcite quench tool of Material Studio. The molecular structures were first subjected to geometric optimization using a maximum iteration of 1000 and energy of 0.01 Kcal/mol. Modeling was achieved using the Condensed phase Optimized Molecular Potentials for Atomistic Simulation Studies (COMPASS) force field including smart algorithm. The temperature was maintained at 298*K* using the Andersen thermostat having NVE microcanonical ensemble, 1fs step time and 5ps total simulation time were used and the number of steps were 5000. The Fe (110) slab was chosen for the simulation with a simulation box of dimension 30 × 25 × 29 Å and periodic boundary conditions to simulate representative section of the interface [36].The simulation box consist of Fe (1 1 0), electrolytic systems [(H_2O, H_3O^+, Cl^-) and (H_2O, H_3O^+ and SO_4^-)] and inhibitor molecules. The configuration of the lower layer of the Fe slab was constraint to the lager position, although the other degrees of freedom were relaxed before the optimization of the Fe (1 1 0) was done which was further increased to 12 × 8 supercell. Quenching was done every 250 steps.

The results of interaction mechanism between the inhibitor and the metal surface in the presence of the following molecules H_2O, H_3O^+, Cl^- and SO_4^- performed with molecular dynamic simulation are presented in Figure 9, Figure 10 and Table 4.

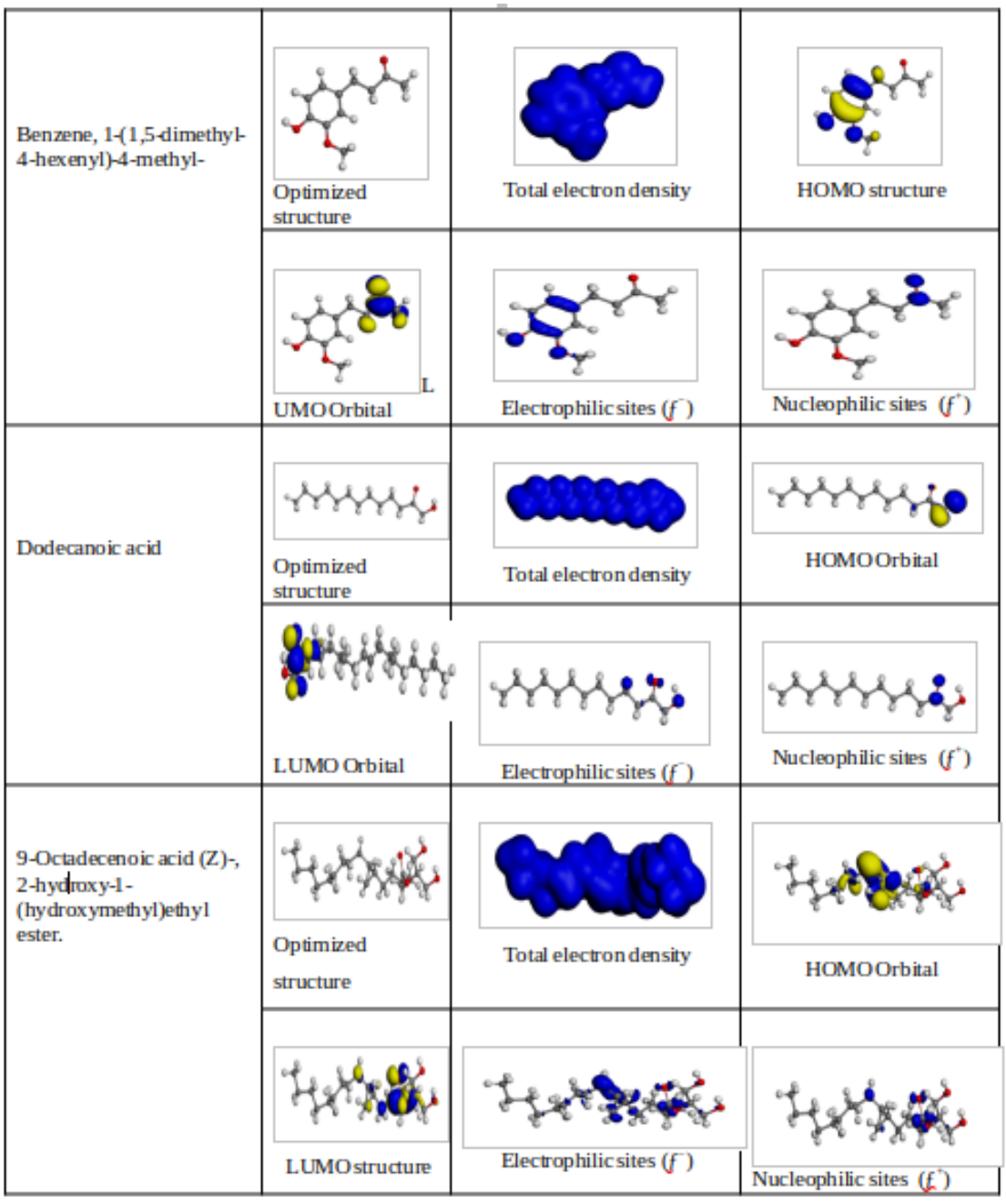

Figure 8: Electronic properties of benzene, 1-(1,5-dimethyl-4-hexenyl)-4- methyl,dodecanoic acid and 9-Octadecenoic acid (Z)-2-hydroxy-1- (hydroxymethyl)ethyl ester

The results in Figure 8 and 9 show that the inhibitor maintained a flat-lying adsorption orientation on the surface of the metal as a result of the delocalization of the electron density all over the molecule. This type of orientation is known to improve close contact between the inhibitor and the metal surface. In other to study the effect of the different acid corrodent on the adsorption energy, the solvation particles H_2O, H_3O^+, Cl^-) and H_2O, H_3O^+ and SO_4^-)] were packed into the simulation box using the amorphous cell tool of the material studio 7.0 modeling and simulation software. The level of interaction between each inhibitor molecule and the metal surface was quantified by evaluating the energy of interaction energy equation (10):

$$\text{Interaction Energy} = E_{\text{total}} - \left(E_{Fe+\text{solvation particles}} - E_{\text{inhibitor}}\right), \quad (10)$$

where E_{total}, $E_{\text{Fe+solvent particles}}$ and $E_{\text{Inhibitor}}$ corresponds to the total energy of the Fe (110)/$E_{\text{Fe+solvent particles}}$ couple, Energy of the Fe slab in addition to the solvent particles and the energy of the inhibitor molecule respectively, the solvation particles refer to either H_2O, H_3O^+, Cl^-) and H_2O, H_3O^+ and SO_4^-, a negative value of the interaction energy is an indication that the molecule possess a stable adsorption structure, all the molecules studied showed negative values which accounts for

Table 4: Calculated quantum chemical properties for the most stable configurations of the selected ZO constituents

Quantum chemical parameter		Benzene, 1-(1,5-dimethyl-4-hexenyl) -4-methyl-	Dodecanoic acid	9-Octadecenoic acid (Z)-, 2-hydroxy-1-(hydroxymethyl) ethyl ester
E_{HOMO} (eV)		-5.0347	-5.7252	-3.3152
E_{LUMO} (eV)		-1.7278	-2.0098	-2.9711
Energy gap (ΔE)		3.3069	3.7154	0.3440
Electron charge transfer (ΔN)		1.0943	0.8431	11.2051
Absolute hardness (η)		1.65375	1.8577	0.1721
Absolute electronegativity (χ)		3.3813	3.8675	3.1432
Absolute softness (σ)		0.6048	0.5383	5.8106
Interaction energy (Kcal/mol)	HCl	-117.82	-172.46	-167.81
	H_2SO_4	-167.98	-145.35	-355.55

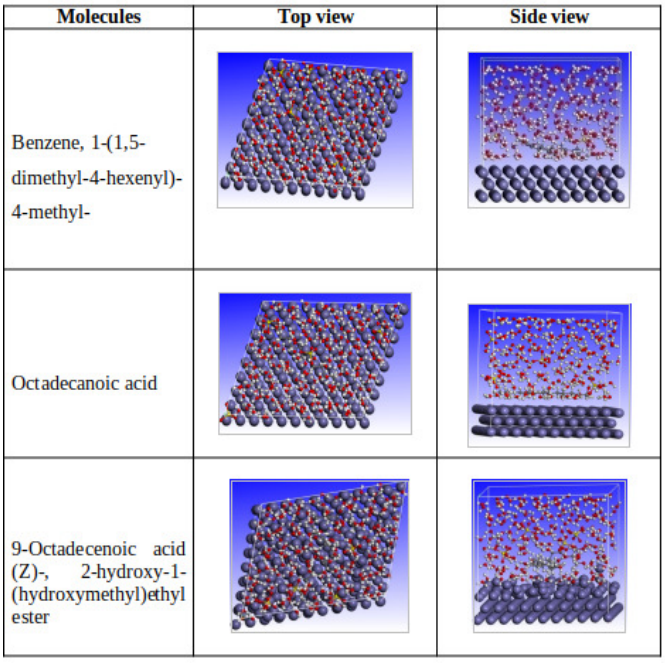

Figure 9: Depiction of the side and top views revealing suitable configurations for adsorption of ZO constituents on Fe (110) surface in H_2SO_4 solution

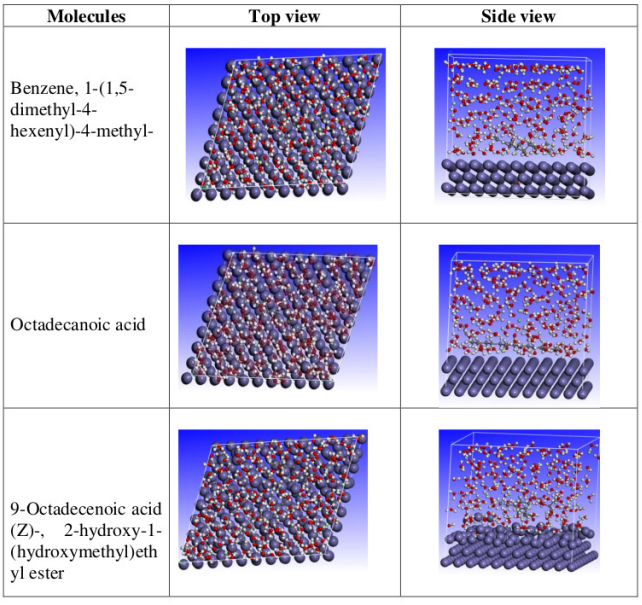

Figure 10: Depiction of the side and top views revealing suitable configurations for adsorption of ZO molecules on Fe (110) surface in 1.0 M HCl acid solution

the inhibition efficiencies obtained in the experimental results.. The large interaction energy (-355.5Kcal/mol) observed for 9-Octadecenoic acid (Z)-, 2-hydroxy-1-(hydroxymethyl)ethyl ester 0.5 M H_2SO_4 mirrors its ability to adsorb better on the metal surface than the other constituents which agrees with the quantum chemical computation result.

4. CONCLUSION

The corrosion inhibition study revealed that the ethanol extract of *Zingiber officinale* efficiently inhibited the corrosion of mild steel induced on 1.0 M HCl and 0.5 M H_2SO_4 acid solution respectively. The PDD results showed that *Zingiber officinale* is a mixed type corrosion inhibitor for mild steel in both acidic solutions while EIS results revealed that *Zingiber officinale* adsorbed on the surface of mild steel indicating the evidence of metal protection. Also, GC-MS results revealed that extract of *Zingiber officinale* contains twenty-three (23) compounds of which three (3) compounds namely; Benzene, 1-(1,5-dimethyl-4-hexenyl)-4-methyl-, Octadecanoic acid and 9-Octadecenoic acid (Z)-, 2-hydroxy-1-(hydroxymethyl)ethyl ester were used for computational studies. Quantum chemical calculation results revealed the positions of quantum chemical descriptors and indicators respectively of the active inhibitor

molecule while the molecular dynamic simulation results provided the binding energy of interaction between the active inhibitor molecule and metal surface. Finally, it observed that extract of ZO exhibited effective corrosion inhibition of mild steel induced in HCl and H_2SO_4 acid solution due to presence of active inhibitive molecule presence in ZO extract.

Acknowledgement

The authors wish to acknowledge Dr Chidiebere of the Department of Science Laboratory Technology, Federal University of Technology Owerri and Dr.C. E. Duru of the Department of Chemistry, Imo State University, Owerri. Imo State Nigeria, West Africa for his immense contribution to the success of this work.

References

[1] T. Popoola, A. S. Grema, G. K. Latinwo, B. Gutti & A. S. Balogun, "Corrosion problems during oil and gas production and its mitigation", International Journal of Industrial Chemistry **35** (2013) 2228, https://doi.org/10.1186/2228.

[2] M. H. Hassan & A. M. Abdullah, "Corrosion of general oil-field grade steel in CO2 environment an update in the light of current understanding", International journal of electrochemical science **12** (2017) 4277, doi: 10.20964/2017.05.12.

[3] M. V. Fiori-Bimbi, P. E. Alvarez, H. Vaca, & Gervasi C. A., "Corrosion inhibition of mild steel in HCl solution by peptin", Corros Science **92** (2015) 192.

[4] B. T. Ogunyemi & B. K. Ojo, "Corrosion inhibition potential of thiosemicarbazide derivatives on aluminium: Insight from molecular modeling and QSAR Approaches", J. Nig. Soc. Phys. Sci. **5** (2023) 915.

[5] G. Sigircik, T.Tuken & M. Erbil, "Assessment of the efficiency of 3, 4-diaminobenzonitrile against the corrosion of steel", Corros Science **102** (2016) 437.

[6] S. C. Nwanonenyi, I. C. Madufor, P. C. Uzoma & I. C. Chukwujike, "Corrosion inhibition of mild steel in sulphuric acid environment using millet starch and potassium iodide", Int. Research J. of Pure & Applied Chemistry **2** (2016) 1, DOI: 10.9734/IRJPAC/2016/27881.

[7] S. C. Nwanonenyi, I. O. Arukalam, H. C. Obasi, U. L. Ezeamaku, I. O. Eze, I. C. Chukwujike and M. A. Chidiebere, "Corrosion inhibitive behavior and adsorption of millet (*Panicum miliaceum*) starch on mild steel in hydrochloric acid environment", J. Bio Tribo Corros **3** (2017) 54, DOI 10.1007/s40735-017-0115.

[8] A. H. Al-Moubaraki, A. Chaouiki, J. M. Alahmari, W. A. Al-Hammadi, E. A. Noor, A. A. Al-Ghamdi & Y. G. Ko, "Development of Natural Plant Extracts as Sustainable Inhibitors for Efficient Protection of Mild Steel: Experimental and First-Principles Multi-Level Computational Methods", Materials (Basel) **23** (2022) 8688, doi: 10.3390/ma15238688.

[9] C. C. Aralu, H. O. Chukwuemeka-Okorie & K. G. Akpomie, "Inhibition and adsorption potentials of mild steel corrosion using methanol extract of *Gongronemalatifoliuim*", Appl Water Sci. **12** (2021) 2021.

[10] S. Mo, H. Q. Luo & N. B. Li, "Plant extracts as green corrosion inhibitors for steel in sulphuric acid", Chem. **70** (2016) 1131, doi.org/10.1515/chempap-2016-0055.

[11] C. B. Adindu, E. E. Oguzie & M. A. Chidiebere, "Corrosion inhibition and adsorption behavior of extract of *Funtumiaelastica* on mild steel in acidic solution", International Letters of Chemistry, Physics and Astronomy **66** (2016) 119.

[12] T. O. Martins, E. A. Ofudje, A. A. Ogundiran, O. A.Ikeoluwa, O. A. Oluwatobi, E. F. Sodiya & O. Ojo, "Cathodic corrosion inhibition of steel by *Musa paradisiaca* leave extract", J. Nig. Soc. Phys. Sci. **4** (2022) 740.

[13] H. FBMS, E. I. Attari, A. ElBribri & L. Mhaidra, "Synthesis and anticorrosion for carbon steel of 4-amino- 3,5 Bis (4-Hydroxy-3-methoxy)-1,2.4 Triazole in hydrochloric acid solution", *American Journal of Engineering Research* **4** (2015) 44.

[14] K. K. Adama & I. B.Onyeachu, "The corrosion characteristics of SS316L stainless steel in a typical acid cleaning solution and its inhibition by 1-benzylimidazole: Weight loss,electrochemical and SEM characterizations", J. Nig. Soc. Phys. Sci. **4** (2022) 214.

[15] M. Cui & X. Li, "Nitrogen and sulfur Co-doped carbon dots as ecofriendly and effective corrosion inhibitors for Q235 carbon steel in 1 M HCl solution", RSC Advances **11** (2021) 21607, doi: 10.1039/d1ra02775a.

[16] M. Faiz, A.Zahari, K. Awang & H. Hussin, "Corrosion inhibition on mild steel in 1 M HCl solution by *Cryptocaryanigra* extracts and three of its constituents (alkaloids)", RSC Adv. **10** (2020) 6547, Doi: 10.1039/c9ra05654h.

[17] F. O. Kolawole, S. K. Kolawole, O. M. Olugbemi & S. B. Hassan, *Green Corrosion Inhibitory Potentials of Cassava Plant (Manihotesculenta Crantz) Extract Nanoparticles (CPENPs) in Coatings for Oil and Gas Pipeline*, In (Ed.) Corrosion Inhibitors, IntechOpen, (2019), `https://doi.org/10.5772/intechopen.79221`.

[18] S. Wan, H. Wei, R. Quan, Z. Luo, H. Wang, B. Liao & X. Guo, "Soybean extract firstly used as a green corrosion inhibitor with high efficacy and yield for carbon steel in acidic medium", Industrial Crops and Products **187** (2022) 115354, `https://doi.org/10.1016/j.indcrop.2022.115354`.

[19] L. Feng, S. Zhang, L. Hao, H. Du, R. Pan, G. Huang & H. Liu, "Cucumber (Cucumissativus L.) Leaf Extract as a Green Corrosion Inhibitor for Carbon Steel in Acidic Solution",Electrochemical, Functional and Molecular Analysis. Molecules **27** (2022) 3826. `https://doi.org/10.3390/molecules27123826`

[20] A. Kadhim, N. Betti,H. A. Al-Bahrani, M. K. S. Al-Ghezi, T. Gaaz, A. H. Kadhum & A. Alamiery, "A mini review on corrosion, inhibitors and mechanism types of mild steel inhibition in an acidic environment", International Journal Corrosion Scale Inhibition **3** (2021) 861.

[21] N. E. Chile, et al. "Theoretical study and adsorption behavior of urea on mild steel in automotive gas oil (AGO) Medium",Lubricants **10** (2022) 157, https://doi.org/10.3390/lubricants10070157.

[22] S. Malhotra & A. P. Singh, "Medicinal properties of ginger (Zingiberoficinale Rosc.)",Nat. Prod. Radi. **2** (2003) 296, `http://hdl.handle.net/123456789/12292`

[23] M. H. Shahrajabian, W.Sun & Q. Cheng, "Clinical aspects and health benefits of ginger (*Zingiber officinale*) in both traditional Chinese medicine and modern industry", ActaAgricultural Scandinavica B-Soil and Plant Science **69** (2019) 6.

[24] N. Jayaraman, P. Punniyakotti, A. U. Nanthini, G. Benelli, M. Kadarkarai & R, Aruliah, "Ginger extract as green biocide to control microbial corrosion of mild steel", Biotech **7** (2017) 133, `https://doi.org/10.1007/s13205-017-0783-9`

[25] N. D. Suma & S. Sreeja, "Adsorption behaviour of Ginger powder on Mild steel corrosion inPotable water", Journal of Material and Environmental Science **8** (2019) 778.

[26] A. S. Fouda, A. A. Nazeer & M. Fakih, "Ginger Extract as Green Corrosion Inhibitor for Steel in Sulfide Polluted Salt Water", Korean chemical Society **57** (2013) 272, `https://doi.org/10.5012/jkcs.2013;57.2.272`.

[27] C. B. Adindu, M. A. Chidiebere, F. C. Ibe, C. E. Ogukwe & E. E. Oguzie, "Protecting Mild Steel from Acid Corrosion Using Extract from *Ocimumgratissimum* Leaves", International Letters of Chemistry, Physics and Astronomy **73** (2017) 9, doi:10.18052/www.scipress.com/ILCPA.73.9.

[28] M. A. Chidiebere, N. Lebe, C. B. Adindu, K. L. Oguzie, B. Okolue, B. E. Onyeachu & E. E. Oguzie, "Inhibition of Acid Corrosion of Mild Steel Using Delonixregia Leaves Extract", International Letters of Chemistry, Physics and Astronomy **69** (2017) 74.

[29] B. Adindu, C. E. Ogukwe, F. Eze & E. Oguzie, Exploiting the Anticorrosion Effects of *Vernonia Amygdalina* Extract for Protection of Mild Steel in Acidic Environments, Journal of Electrochemical Science and Technology **74** (2016) 251.

[30] E. E. Oguzie, C. B. Adindu, C. K. Enenebeaku, C. E. Ogukwe, M. AChidiebere & K. L. Oguzie, "Natural Products for Materials Protection: Mechanism of Corrosion Inhibition of Mild Steel by Acid Extracts of Piper guineense", ACS Journal of physical Chemistry C **116** (2012) 13603, dx.doi.org/10.1021/jp300791s.

[31] T. Jianhong, G. Lei, W.Dan, W.Shanfei, Y. Rongrong, Z. Fan, K. Savas, " Electrochemical and Computational studies on the corrosion inhibi-

tion of mild Steel by 1-Hexadecyl-3-methylimidazolium Bromide in HCl medium",International Journal of electrochemical Sciences **15** (2020) 1893, doi: 10.20964/2020.03.36.

[32] F. A. Khalida, B. A. Shaima, Z. M. Ayad, A. A. Ahmed, K. A. Talib, A. M. Salam, H. K. Abdul Amir & B. Abu, "Synthesis, inhibition effects and quantum chemical studies of a novel coumarin derivative on the corrosion of mild steel in a hydrochloric acid solution",BMC Chemistry **10** (2016) 23.

[33] B. Umar, A. Uzairu & G.Shallangwa, "Understanding inhibition of steel corrosion by some potent triazole derivatives of pyrimidine through density functional theory and molecular dynamics simulation studies", JOTCSA **6** (2019) 455.

[34] J. Coates, Interpretation of Infrared Spectra, A Practical Approach, in Encyclopedia of Analytical Chemistry R.A. Meyers (Ed.), John Wiley & Sons Ltd, Chichester, (2000).

[35] C. P. Ozoemena & M. Charles, "Computational Modeling and Statistical analysis on the corrosion inhibition of aluminium in nitric acid solution by ethanolic extract of citrus sinesis seed",Global Journal of Pure and Applied Chemistry Research **7** (2019) 25.

[36] I. C. Iwu,R. N. Oze, U. L.Onu, N. Amarachi & A. Ukaoma, "phytochemical and GC-MS analysis of the rhizome of Zingiber officinale plant grown in eastern part of Nigeria", African Journal of Biology and Medical research **11** (2018) 43.

[37] E. .E. Oguzie,K. L. Oguzie, C. O.Akalezi, I. O.Udeze, J. N.Ogbulie, and V. O. Njoku, "Natural Products for Materials Protection: Corrosion and Microbial Growth Inhibition Using Capsicum frutescens Biomass Extracts", ACS Sustainable Chemistry and Engineering, **1** (2013) 214, .doi.org/10.1021/sc300145k.

[38] C. O. Akalezi, C. K. Enenebaku & E. E. Oguzie, "Application of aqueous extracts of coffee senna for control of mild steel corrosion in acidic environments".*Int J IndChem* **3** (2012) 13, `https://doi.org/10.1186/2228-5547-3-13`

[39] U. C. Ibeji, C. D. Akintayo, H. O. Oluwasola & E. O. Akintemi, "Anti-Corrosion potential of the Ortho and ParaSubstituted Schiff Bases of 2-Methoxybenzaldehyde on Fe (110) surface in acid medium: Synthesis, DFT and Molecular Dynamics Studies", Research Square (2022) DOI: `https://doi.org/10.21203/rs.3.rs-1869552/v1`.

[40] R. S. Oguike & O. Oni, "Density Functional Theory of Mild Steel Corrosion in Acidic Media Using Dyes as Inhibitor: Adsorption onto Fe(110) from Gas Phase"Int. J. Res. Chem. Environ. **4** (2014) 177.

[41] R. S. Oguike, A. M. Kolo, A. M. Shibdawa & H. A. Gyenna, "Density Functional Theory of Mild Steel Corrosion in Acidic Media Using Dyes as Inhibitor: Adsorption onto Fe(110) from Gas Phase", ISRN Physical Chemistry **2013** (2013) 175910, `https://doi.org/10.1155/2013/175910`.

[42] A. E. Founda, A. H. El-Ashalany, A. F. Molouk, N. S. Elsheikh & A. S Abousalem, "Experimental and computational chemical studies on the corrosion inhibitive properties of carbonitrile compounds for carbon steel in aqueous solutions", Science Representative **11** (2021) 21672, `https://doi.org/10.1038/s41598-021-00701-z`